

## PDF hosted at the Radboud Repository of the Radboud University Nijmegen

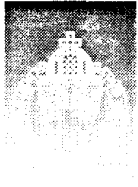
The following full text is a preprint version which may differ from the publisher's version.

For additional information about this publication click this link.

<http://hdl.handle.net/2066/29381>

Please be advised that this information was generated on 2018-07-07 and may be subject to change.

AB

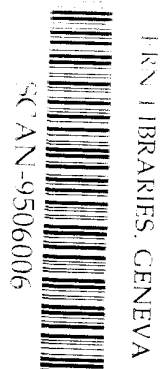


Radboud Universiteit Nijmegen

Nijmegen preprint  
HEN-382  
April 1995

## Angular Dependence of Particle Correlations in $\pi^+/\text{K}^+$ p interactions at 250 GeV/c

EHS-NA22 Collaboration



SW 9523

# Angular Dependence of Particle Correlations in $\pi^+ / K^+ p$ Interactions at 250 GeV/c

EHS-NA22 Collaboration

N.M. Agababyan<sup>h</sup>, I.V. Ajinenko<sup>e</sup>, M.R. Atayan<sup>h</sup>, K. Belous<sup>e</sup>, M. Charlet<sup>d,1</sup>,  
P.V. Chliapnikov<sup>e</sup>, J. Czyzewski<sup>d,2,3</sup>, E.A. De Wolf<sup>a,4</sup>, K. Dziunikowska<sup>b,3</sup>,  
A.M.F. Endler<sup>f</sup>, Z.Sh. Garutchava<sup>g,5</sup>, H.R. Gulkanyan<sup>h</sup>, R.Sh. Hakobyan<sup>h,6</sup>,  
J.K. Karamyan<sup>h</sup>, D. Kisielewska<sup>b,3</sup>, W. Kittel<sup>d</sup>, S.S. Mehrabyan<sup>h</sup>, Z.V. Metreveli<sup>g,6</sup>,  
W. Metzger<sup>d</sup>, K. Olkiewicz<sup>b,3</sup>, F.K. Rizatdinova<sup>c</sup>, E.K. Shabalina<sup>c</sup>, L.N. Smirnova<sup>c</sup>,  
M.D. Tabidze<sup>g</sup>, L.A. Tikhonova<sup>c</sup>, A.G. Tomaradze<sup>g,5</sup>, F. Verbeure<sup>a</sup>, S.A. Zotkin<sup>c,7</sup>

<sup>a</sup> Department of Physics, Universitaire Instelling Antwerpen, B-2610 Wilrijk, Belgium

<sup>b</sup> Institute of Physics and Nuclear Techniques of Academy of Mining and Metallurgy and Institute of Nuclear Physics, PL-30055 Krakow, Poland

<sup>c</sup> Nuclear Physics Institute, Moscow State University, RU-119899 Moscow, Russia

<sup>d</sup> University of Nijmegen/NIKHEF, NL-6525 ED Nijmegen, The Netherlands

<sup>e</sup> Institute for High Energy Physics, RU-142284 Protvino, Russia

<sup>f</sup> Centro Brasileiro de Pesquisas Fisicas, BR-22290 Rio de Janeiro, Brazil

<sup>g</sup> Institute for High Energy Physics of Tbilisi State University, GE-380086 Tbilisi, Georgia

<sup>h</sup> Institute of Physics, AM-375036 Yerevan, Armenia

## Abstract.

A sample of non-diffractive  $\pi^+ p$  and  $K^+ p$  collisions at  $\sqrt{s}=22$  GeV is used to investigate the angular dependence of the particle-particle correlation (PPC) and its asymmetry (PPCA) for soft hadronic data. The results differ strongly from the overall behavior in  $e^+e^-$  data, but agree with that expected for  $e^+e^-$  2-jet data. For the hadronic collisions, the effect depends strongly on the charge configuration of the pairs and on the rapidity range covered. The FRITIOF Monte-Carlo model gives qualitative agreement with the trend of the overall data when Bose-Einstein correlations are included, but differs considerably in the central rapidity region.

<sup>1</sup> EC guest scientist, now at DESY, Hamburg

<sup>2</sup> KUN Fellow from the Jagellonian University, Krakow

<sup>3</sup> Supported by the Polish State Committee for Scientific Research

<sup>4</sup> Onderzoeksleider NFWO, Belgium

<sup>5</sup> Now at UIA, Wilrijk, Belgium

<sup>6</sup> FOM guest at the Univ. of Nijmegen

<sup>7</sup> NWO guest at the Univ. of Nijmegen

## 1. Introduction

In QCD, color coherence manifests itself in an Angular Ordering (AO) of partons produced in the parton shower prior to hadronization [1]. As a result, the angle of each gluon emitted in the shower is smaller than that of its parent. According to local parton-hadron duality (LPHD) [2], color singlet hadrons still carry information on AO of their parent partons after hadronization.

Based on the assumption of LPHD, an investigation of AO has recently been performed on hadronic decays of  $Z^0$  in [3,4]. In such an analysis, particle-particle correlation (PPC) functions<sup>1</sup> are constructed for hadrons in a way analogous to energy-energy correlation functions [5],

$$\text{PPC}(\chi) = \frac{1}{\Delta\chi} \langle 2 \sum_{i < j}^n \frac{1}{\langle n \rangle^2} \delta_{\text{bin}}(\chi - \chi_{ij}) \rangle \quad (1)$$

and their asymmetry

$$\text{PPCA}(\chi) = \text{PPC}(\chi) - \text{PPC}(180^\circ - \chi) \quad (2)$$

where  $\chi_{ij}$  is the angle between tracks  $i$  and  $j$  in the cms, the summation is over all pairs  $ij$  fulfilling  $i < j$ ,  $\langle \rangle$  is the average over all events in the sample,  $n$  is the number of charged tracks in an event and  $\Delta\chi$  is the bin width. The function  $\delta_{\text{bin}}(\chi - \chi_{ij})$  is 1 if  $\chi_{ij}$  and  $\chi$  are in the same bin and 0 otherwise.

The exact shape of  $\text{PPCA}(\chi)$  for hadronic  $e^+e^-$  events at the  $Z^0$  peak turns out to be sensitive to AO in the region  $\chi < 45^\circ$  and clearly favors MC models with AO over those without [3,4], thus supporting the QCD prediction. To be able to interpret these and future results in terms of perturbative QCD, it is useful to compare to collisions *not* dominated by perturbative QCD.

In this paper we, therefore, investigate the behavior of (2) in soft hadronic collisions at  $\sqrt{s} = 22$  GeV. Of course, it is *not* the aim to search for angular ordering in soft collisions, but to *compare* the structure in angular two-particle correlations in terms of  $\chi$  dependence of PPCA in hard and soft collisions. In search for the origin of the structure, the analysis is performed for all charged particles (cc) combined, as well as for the charge configurations  $(--)$ ,  $(+-)$  and  $(++)$ , separately.

## 2. The data

The full experimental set-up of EHS, exposed to a positive meson enriched beam with momentum 250 GeV/c, is described in detail in [6,7]. It consists of an active vertex detector (Rapid Cycling Bubble Chamber filled with  $\text{H}_2$ ) and a down-stream two-lever-arm spectrometer. Tracks of secondary charged particles are reconstructed from hits in the wire- and driftchambers of the spectrometer and from measurement in RCBC. The momentum resolution varies from (1-2)% for tracks reconstructed in RCBC, to (1-2.5)% for tracks reconstructed in the first lever arm and to 1.5% for tracks reconstructed in the full spectrometer.

---

<sup>1</sup>In the present analysis we replace the  $n^2$  used by ALEPH [3] and L3 [4] in (1) by  $\langle n \rangle^2$  to stay consistent with the more commonly used definition of the two-particle correlation function. This difference slightly changes the form of the function, but not the conclusions of the analysis. Note further, that the sign definition of PPCA is inverted in (2) with respect to the definition of [3, 4]. This is done in order to obtain *positive* values for PPCA if the correlation is *positive*.

An event is accepted for analysis if the measured and reconstructed charge multiplicity is the same, charge balance is satisfied, no electron is detected among the secondary tracks and no track is badly reconstructed (and therefore rejected). The loss of events during measurement and reconstruction is corrected for by means of the topological cross section data [7]. Elastic events are excluded. Furthermore, an event is called single-diffractive and excluded from the sample if the total charge multiplicity is smaller than 8 and at least one of the positive tracks has  $|x_F| > 0.88$ . After these cuts, the inelastic non-single-diffractive sample consists of about 59.200  $\pi^+p$  and  $K^+p$  events.

For momenta  $p_{\text{lab}} < 0.7 \text{ GeV}/c$ , the range in the bubble chamber and/or the change of track curvature is used for proton identification.

In addition, a visual ionization scan has been performed for  $p_{\text{lab}} < 1.2 \text{ GeV}/c$  on the full  $K^+p$  and on 62% of the  $\pi^+p$  sample. A positive particle with  $p_{\text{lab}} > 150 \text{ GeV}/c$  is given the identity of the beam particle. Other particles with momentum  $p_{\text{lab}} > 1.2 \text{ GeV}/c$  are not identified in the present analysis and are treated as pions. The  $\pi^+p$  and  $K^+p$  samples are combined into one sample.

### 3. The results

#### 3.1 The PPC distribution

In Fig. 1, PPC is given as a function of the interparticle cms angle  $\chi$  for all pairs of charged particles in our data (full circles). The bin width used here and in the other figures is  $\Delta\chi = 5^\circ$ . In Fig. 1a, our data are compared to the expectation from no correlation (dotted line) and to L3 data [4] (open circles). Non-zero correlations exist for both data sets. For both, the general structure consists in a maximum at small and one at large angles and a broad minimum around  $90^\circ$ . For the  $e^+e^-$  data at the  $Z^0$ -mass, this structure is far more pronounced than for hadron-hadron collisions at  $\sqrt{s} = 22 \text{ GeV}$ .

In Fig. 1b, our data are compared to the expectation from the FRITIOF Monte-Carlo model [8], version 7.02 [9]. To include BE correlations, we use the algorithm developed in JETSET 7.3 [10] for pions which are directly produced or are decay products from short-lived resonances<sup>2</sup>. Exponential parametrization in the four-momentum difference  $Q = [-(p_1 - p_2)^2]^{1/2}$  is applied. In [11] it has been shown that the maximal value of  $\lambda = 1$  is needed for the correlation strength. The value of radius  $r = 0.8 \text{ fm}$  used here is that measured in our experiment [12]. Events generated with the model are subject to the same selection criteria as the real data. The dashed line in Fig. 1b shows FRITIOF without Bose-Einstein (BE) correlations, the solid line FRITIOF with BE correlations. Including BE in FRITIOF enhances the correlation for angles  $\chi < 45^\circ$  and reduces it around  $\chi = 90^\circ$ . Both models reproduce the general trend of the PPC distribution, but underestimate the correlation at angles between  $30^\circ$  and  $135^\circ$ .

#### 3.2 Comparison of PPCA to $e^+e^-$ collisions

In Fig. 2a, the asymmetry PPCA is plotted as a function of the angle  $\chi$  for the L3 data [4] (in the L3 normalization). A peak is observed at small angles, a minimum at  $25^\circ$  and a broad shoulder at larger angles. As shown in [4], JETSET with angular ordering [10] is describing this distribution perfectly well. The curves are due to the same JETSET, but enriched in

<sup>2</sup>All states with life time longer than the  $K^*(892)$  are considered to be long-lived [10].

2-jet events by the JADE jet-finding algorithm [13] with  $y_{\text{cut}} = 0.08$  (dashed) and  $y_{\text{cut}} = 0.02$  (full). One can see how the minimum observed in the full L3 sample at  $25^\circ$  shifts towards smaller angles and becomes considerably deeper the smaller  $y_{\text{cut}}$ , i.e. the more one restricts the analysis to 2-jet events.

In Fig. 2b we show our data (full circles). Quite a dramatic difference is observed with the L3 data given in Fig. 2a, in particular at  $\chi < 20^\circ$  where PPCA is positive for L3 and negative for NA22. The full line is the same as the full line in Fig. 2a, but now in  $\langle n \rangle^2$  normalization. It roughly shows the same feature as the NA22 data. So, the positive PPCA at small  $\chi$  in L3 is due to higher jet multiplicities. This can be explained from the suppression of tracks at  $180^\circ$  due to the angular opening between jets 2 and 3.

### 3.3 Charge dependence

In recent studies on our data [14,15], it has been shown that the structures in particle correlations depend strongly on the charge combination of the particles in question. To obtain more insight into the origin of the structure of  $\text{PPCA}(\chi)$  we, therefore, compare in Fig. 3 the NA22 distribution for all charged particles (Fig. 3a) to that for the three possible charge combinations  $(--)$ ,  $(+-)$  and  $(++)$  (Figs. 3b-d, respectively). Indeed, the behavior is very different for the different cases:

- For all pairs (Fig. 3a), the PPCA is negative in the region  $\chi \leq 20^\circ$ .
- For  $(--)$  pairs (Fig. 3b), no angular dependence is observed in the data and PPCA is in agreement with zero over the full  $\chi$  region.
- For  $(+-)$  pairs (Fig. 3c), the PPCA is positive for the full angular region except for very small  $\chi$ . It is well known that decay of many states ( $\rho^0, \eta, \eta', \dots$ ) strongly affects the  $(+-)$  correlations [11,14].
- For  $(++)$  particle combinations (Fig. 3d), the PPCA is negative for the full  $\chi$  region, but close to zero for the region  $\chi \geq 45^\circ$ . This and the difference with  $(--)$  can be explained by the positive charge of the leading particles in our experiment (see below).

For all charge combinations, FRITIOF with BE correlations gives reasonably good agreement with the data in Fig. 3.

### 3.4 Central rapidity region

To reduce the influence of beam and target particles, we show in Fig. 4 the  $\text{PPCA}(\chi)$  distribution in the restricted kinematical (central) region  $-2 < y < 2$ , again for data (full circles) and FRITIOF (lines). The negative correlation observed at  $\chi \leq 20^\circ$  for all pairs in Fig. 3a and  $(++)$  pairs in Fig. 3d disappears in the central region. This indicates that in hadron-hadron collisions PPCA and its shape strongly depends on the influence from the leading charges. So, either the agreement with  $e^+e^-$  2-jet events found in Fig. 2 is accidental or a similar charge effect is present also there. Due to the opposite charge of the primary  $q\bar{q}$  pair, this effect would show up in  $(+-)$  correlations, of course.

Even though FRITIOF with BE correlations leads to better agreement with the data than without, the model only describes the shape of the PPCA, but underestimates its magnitude

for all charge combinations. This underestimation is connected to a more general failure of the model to describe the correlation effects in our data [e.g. 14,15], which cannot be cured by simple retuning of the model.

#### 4. Conclusions

The angular dependence of the particle-particle correlation asymmetry has been studied for the first time on soft hadron-hadron collisions. It differs strongly from the overall behavior of  $e^+e^-$  data, but is in qualitative agreement with that of  $e^+e^-$  2-jet Monte Carlo. For hadronic data, the PPCA function is very different for the various charge configurations. This should be checked in the  $e^+e^-$  data. The FRITIOF model with Bose-Einstein correlations leads to reasonable agreement with the shape of the data, but the magnitude of the correlations is underestimated in the central rapidity region.

#### Acknowledgements

It is a pleasure to thank the EHS coordinator L. Montanet and the operating crews and staffs of EHS, SPS and H2 beam, as well as the scanning and processing teams of our laboratories for their invaluable help with this experiment. We are grateful to the III. Physikalisches Institut B, RWTH Aachen, Germany, the DESY-Institut für Hochenergiephysik, Berlin-Zeuthen, Germany, the Department of High Energy Physics, Helsinki University, Finland, and the University of Warsaw and Institute of Nuclear Problems, Poland for early contributions to this experiment. This work is part of the research programme of the "Stichting voor Fundamenteel Onderzoek der Materie (FOM)", which is financially supported by the "Nederlandse Organisatie voor Wetenschappelijk Onderzoek (NWO)". We further thank NWO for support of this project within the program for subsistence to the former Soviet Union (07-13-038).

#### References

1. Yu.L. Dokshitzer, V.A. Khoze, A.H. Mueller and S.I. Troyan: *Rev. Mod. Phys.* 60 (1988) 373
2. Ya.I. Azimov, Yu.L. Dokshitzer, V.A. Khoze, S.I. Troyan: *Z. Phys.* C27 (1985) 65
3. Mokhtar A. Chmeissani: Study of Angular Ordering in the Hadronic Decays of the  $Z^0$ , ALEPH internal note, 93-097, PHYSICS 93-79 (1993)
4. A.A. Syed, *Nucl. Phys. B (Proc. Suppl.)* 39B,C (1995) 157 and Ph.D Thesis, Univ. of Nijmegen, 1994; W. Metzger, *Proc. XXVII Int. Conf. on High Energy Physics Glasgow 1994* (IOP Publishing 1995) p.1293;  
M. Acciarri (L3 Coll.): Evidence for gluon interference in hadronic Z decays, *subm. to Phys. Lett. B.*
5. C. Louis Basham et al.: *Phys. Rev. Lett.* 41 (1978) 1585
6. M. Aguilar-Benitez et al.: *Nucl. Instrum. Methods* 205 (1988) 79
7. M. Adamus et al. (NA22 Coll.): *Z. Phys.* C32 (1986) 475
8. B. Andersson, G. Gustafson, B. Nilsson-Almqvist: *Nucl. Phys.* B281 (1987) 289
9. B. Andersson, G. Gustafson and Hong Pi: *Z. Phys.* C57 (1993) 485
10. T. Sjöstrand and M. Bengtsson, *Computer Phys. Comm.* 43 (1987) 367 and T. Sjöstrand: CERN preprint: CERN-TH.6488/92

11. P. Abreu et al. (DELPHI Coll.): Z. Phys. C63 (1994) 17
12. N. Agababyan et al. (NA22 Coll.): Z. Phys. C59 (1993) 405
13. W. Bartel et al.: Z. Phys. C33 (1986) 23 and W. Bethke et al.: Phys. Lett. 213B (1988) 235.
14. I.V. Ajinenko et al. (NA22 Coll.): Z. Phys. C61 (1994) 567
15. V.V. Aivazyan et al. (NA22 Coll.): Z. Phys. C51 (1991) 167; N.M. Agababyan et al. (NA22 Coll.): Phys. Lett. B332 (1994) 458.



## Figure Captions

- Fig. 1 Dependence of PPC on the angle  $\chi$  for  $\pi^-/K^-p$  collisions at  $\sqrt{s} = 22$  GeV (full circles) compared a) to the expectation from no correlation (dotted) and to the L3 data (open circles) and b) to FRITIOF Monte Carlo results with and without Bose-Einstein correlations (lines). The L3 data are renormalized to  $\Delta\chi$  expressed in degrees.
- Fig. 2 Dependence of PPCA on the angle  $\chi$  for b)  $\pi^+/K^+p$  collisions at  $\sqrt{s} = 22$  GeV (full circles) compared to a) that for 92 GeV  $e^+e^-$  collisions [4] (open circles). Also shown are JETSET Monte Carlo results with a restriction to 2-jet events selected by the JADE jet-finding algorithm with  $y_{cut} = 0.08$  (dashed line) and 0.02 (full line). The L3 data are renormalized to  $\Delta\chi$  expressed in degrees and plotted in our sign convention. The L3 data and JETSET results in Fig. 2a are given in the  $n^2$  normalization, the NA22 data and the full line in 2b) in the  $\langle n \rangle^2$  normalization of the correlation function.
- Fig. 3 Dependence of PPCA on the angle  $\chi$  for different charge combinations, for NA22 data (full circles) and for FRITIOF with and without Bose-Einstein correlations (lines).
- Fig. 4 Same as for Fig. 3, but for the central region  $-2 < y < 2$ .

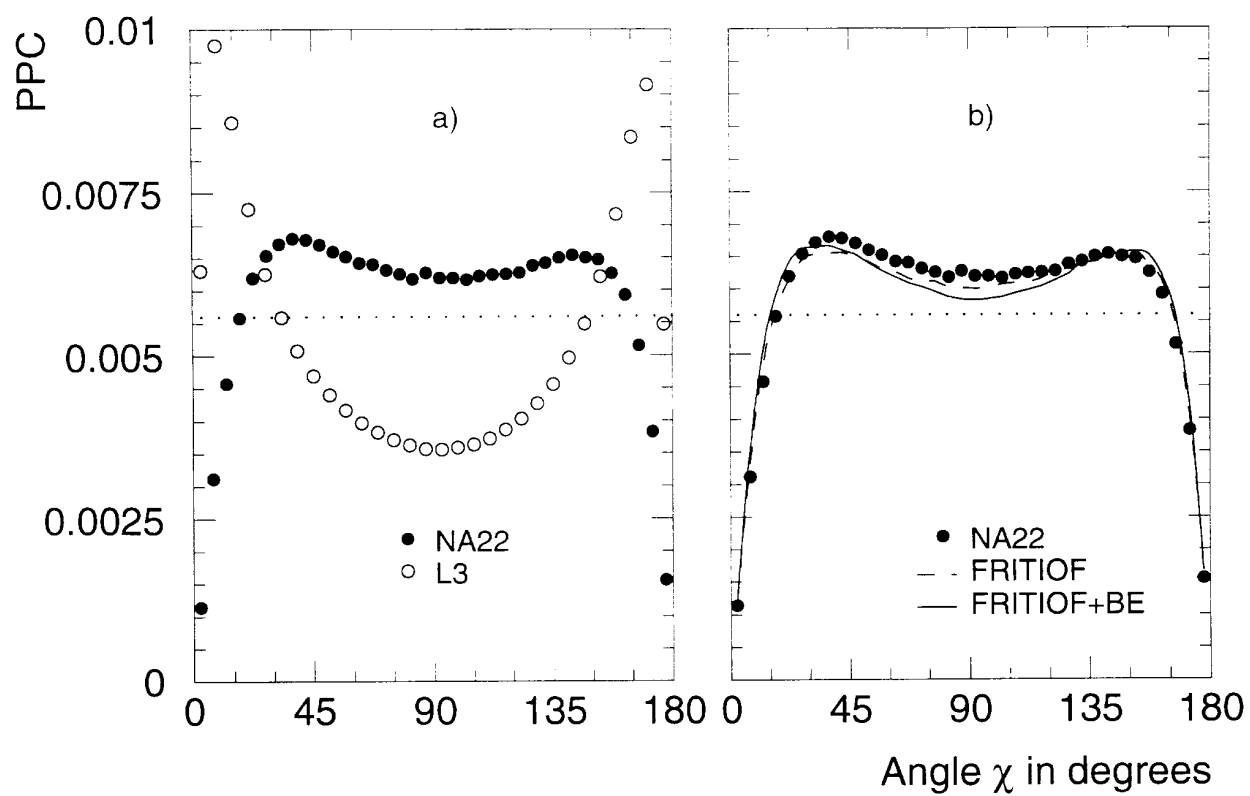


Fig. 1

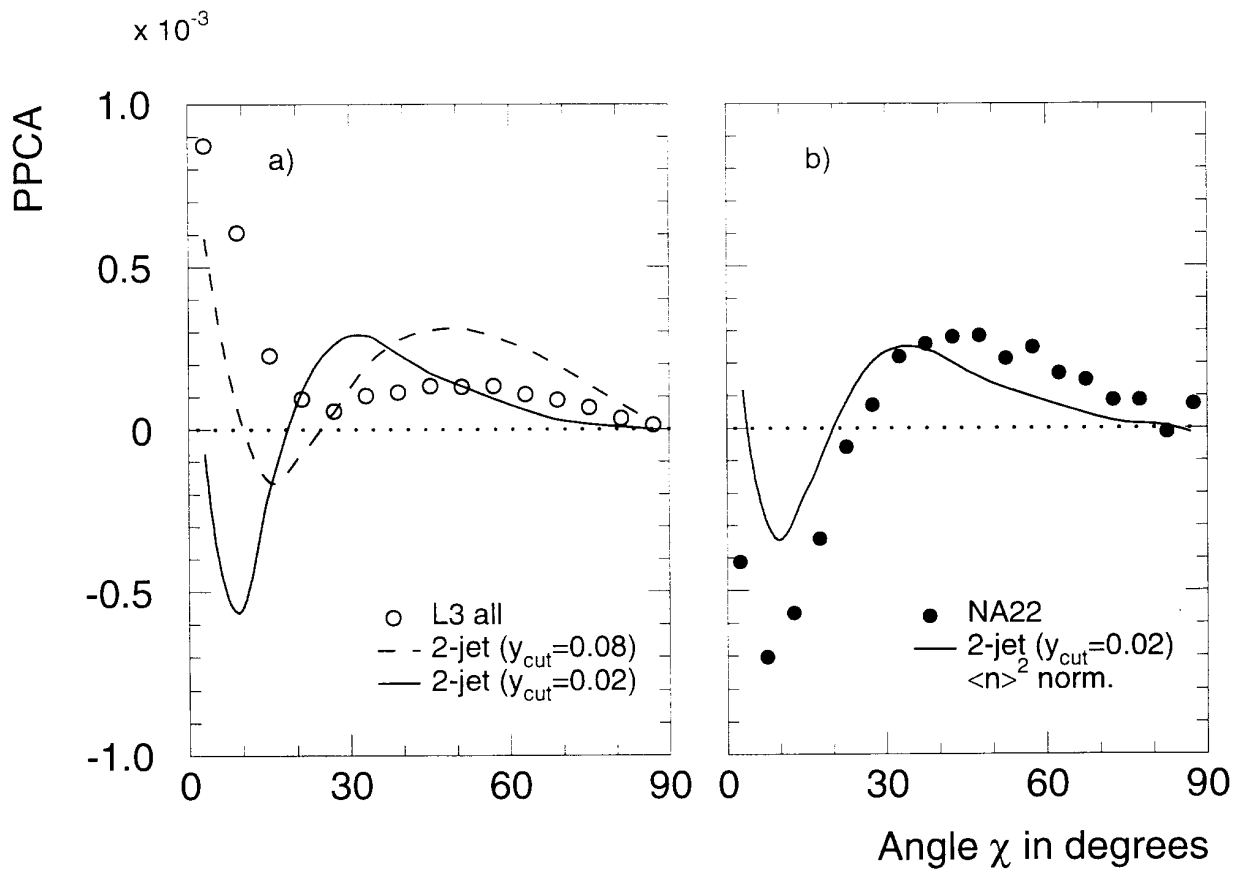


Fig. 2

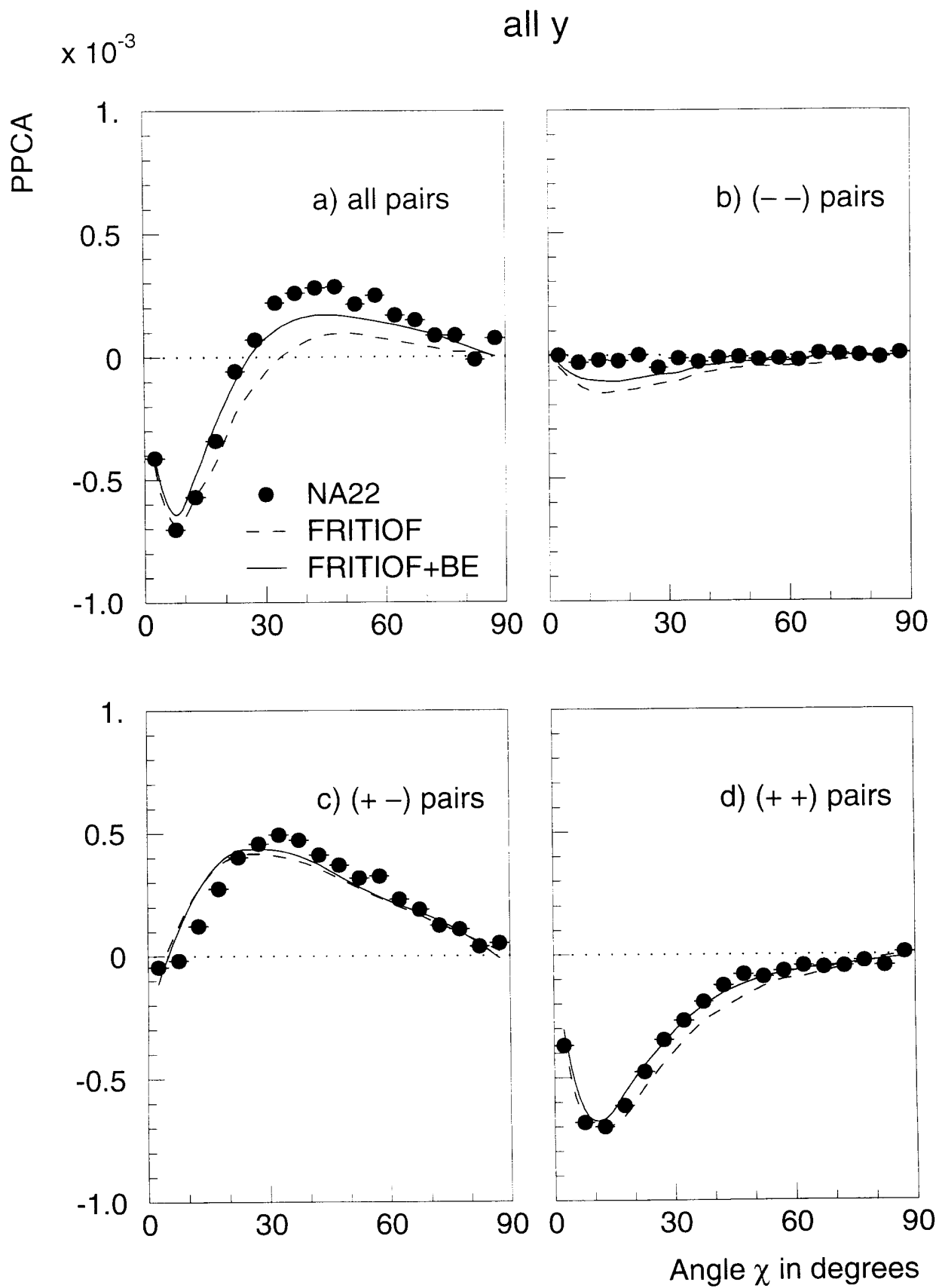


Fig. 3

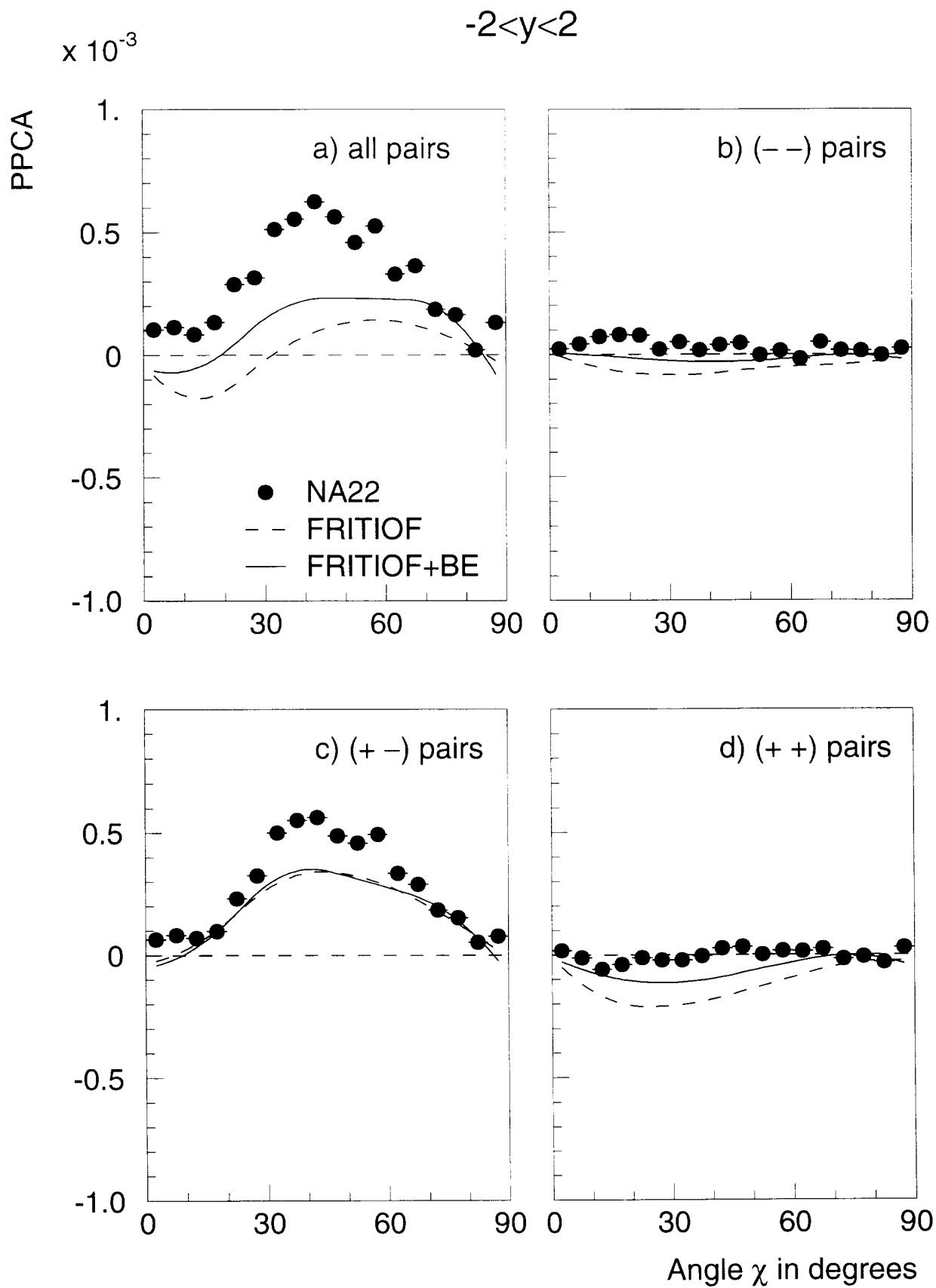


Fig. 4